Journal of Alloys and Compounds 446–447 (2007) 188–194

Journal of ALLOYS AND COMPOUNDS

www.elsevier.com/locate/jallcom

La(TM)$_5$ hydrides (TM = Fe, Co, Ni): Theoretical perspectives

J.F. Herbst*, L.G. Hector Jr.

Materials and Processes Laboratory, General Motors Research and Development Center,
Mail Code 480-106-224, Warren, MI 48090-9055, USA

Received 13 September 2006; accepted 1 December 2006

Abstract

Systematic theoretical results for La(TM)$_5$H$_n$ materials with TM one of the magnetic transition metals Fe, Co, or Ni are discussed. For TM = Co, Ni the antecedent LaCo$_5$ and LaNi$_5$ intermetallics and hydrides are well known. While no La–Fe compounds exist, LaFe$_5$ hydrides are predicted to form by both Miedema's phenomenological model as well as by first-principles density functional theory (DFT) for several prototype crystal structures. Enthalpies of formation and saturation hydrogen contents derived from Miedema's model and DFT are compared. Our phonon calculations for LaCo$_5$ and LaCo$_5$H$_4$ yield new information on their crystal structures.

Keywords: Rare-earth compounds; Hydrogen absorbing materials; Metal hydrides; Electronic structure; Enthalpy

1. Introduction

As a consequence of their numerous representatives and opulent variety of properties the AB$_5$ compounds and their hydrides have received considerable scientific and technological attention over a lengthy period. Gaps in our fundamental knowledge of these systems remain, however, among them the energetics of phase formation and structural issues. Here we focus on a small subset, the La(TM)$_5$H$_n$ materials having ferromagnetic Fe, Co, or Ni as the transition metal (TM) component. LaNi$_5$, LaCo$_5$, and hydrides of them are well known, with LaNi$_5$H$_n$ especially well studied in view of its desirable hydrogen sorption characteristics. We compare enthalpies of formation from both Miedema's semiempirical model and density functional theory (DFT), including vibrational energy contributions in the latter. Our phonon calculations for LaCo$_5$ and LaCo$_5$H$_4$ reveal new insights on their crystal structures. While neither LaFe$_5$ nor any other La–Fe intermetallic forms, Miedema's model and preliminary DFT work strongly suggest the existence of a LaFe$_5$ hydride.

2. Miedema's model

Miedema and co-workers formulated a highly successful semiempirical model for the enthalpy of formation ΔH of binary A–B alloys, with a principal focus on those having at least one TM component [1]. $\Delta H(\mathrm{A}_{c_\mathrm{A}}\mathrm{B}_{c_\mathrm{B}})$ is derived from a set of parameters for each of the elemental constituents; no structural information is involved. Results for the parent compounds of interest here are given in Table 1. The model correctly predicts the formation of LaNi$_5$, LaCo$_5$, and the absence of LaFe$_5$. ΔH_calc(LaNi$_5$) is in reasonable agreement with experiment, but ΔH_calc(LaCo$_5$) severely underestimates the magnitude of the measured value; it is interesting to note that in contrast to LaNi$_5$, LaCo$_5$ undergoes a eutectoid decomposition below ~600 °C [4]. Moreover, $\Delta H_\mathrm{calc}(\mathrm{La}_{0.5}\mathrm{Fe}_{0.5}) = +6.4$ kJ/mole La$_{0.5}$Fe$_{0.5}$ at the equiatomic composition, a value indicating [1] that no La–Fe binary phases whatsoever form, in accord with observation.

Miedema's original model was generalized to binary AH$_x$ and ternary AB$_n$H$_{x+y}$ hydrides of known hydrogen content and having B:A ratios $n = 1, 2, 3, 5$ [5]; ΔH of the latter is expressed as

$$\Delta H(\mathrm{AB}_n\mathrm{H}_{x+y}) = \Delta H(\mathrm{AH}_x) + \Delta H(\mathrm{B}_n\mathrm{H}_y) - (1-\mathrm{F})\Delta H(\mathrm{AB}_n) \quad (1)$$

To enable an estimate of the hydrogen fraction the model was extended recently to arbitrary hydrogen content as well as to

---

* Corresponding author. Tel.: +1 586 986 0580; fax: +1 586 986 3091.
E-mail address: jan.f.herbst@gm.com (J.F. Herbst).

0925-8388/$ – see front matter © 2006 Elsevier B.V. All rights reserved.
doi:10.1016/j.jallcom.2006.12.003

Table 1
Enthalpies of formation ΔH of $LaTM_5$ intermetallic compounds calculated with Miedema's model and experimental values

	$LaNi_5$	$LaCo_5$	$LaFe_5$
ΔH_{calc}	−141	−89	+24
ΔH_{expt} (298 K)	−159.1[a], −166[b]	−17[b]	–

All ΔH entries in kJ/mole fu (=0.010364 eV/fu; fu = formula unit).

[a] Ref. [2].

[b] Ref. [3].

arbitrary n via the *ansatz* [6]

$$\Delta H(AB_nH_x) = \Delta H(AH_{\alpha(n)x}) + \Delta H(B_nH_{[1-\alpha(n)]x}) - \left[\frac{x}{\beta(n)+x}\right]\Delta H(AB_n) \tag{2}$$

The functions $\alpha(n)$ and $\beta(n)$ are constructed to satisfy several reasonable constraints and to ensure that Eq. (2) reduces to Eq. (1) for $n = 1, 2, 3, 5$ and the (x, y, F) parameter sets of Bouten and Miedema [5]. As in ref. [6], minimization of $\Delta H(AB_nH_x)$, specified per mole AB_nH_x by Eq. (2), provides an estimate x_{calc}^{max} of the maximum hydrogen content. Eq. (2) can also be employed to find x_{calc}^{0} which minimizes the enthalpy per mole H_2, $(2/x)\,\Delta H(AB_nH_x)$. In keeping with the van't Hoff relation [7]

$$\ln p/p_0 = [(2/x)\Delta H(AB_nH_x)]/RT - \Delta S/R \tag{3}$$

x_{calc}^{0} can be identified as the hydrogen content of the hydride in equilibrium with the AB_n parent and H_2 gas along the plateau at lowest pressure in a pressure-composition isotherm experiment. Results are presented in Table 2. In the case of $LaFe_5H_x$, the $\Delta H(LaFe_5)$ term in Eq. (2) was neglected since $LaFe_5$ does not form, so that $\Delta H(LaFe_5H_x)$ represents the enthalpy of formation with respect to La and Fe metals and H_2 gas. For $LaNi_5H_x$ and $LaCo_5H_x$ the predicted hydrogen content x_{calc}^{0} of the first-plateau hydride is in good proximity to x_{expt}^{0} but $|\Delta H_{expt}|$ is underestimated; x_{calc}^{max} tends to the hydrogen content x_{expt}^{max} at the highest pressure observed. The model predicts the existence of $LaFe_5H_x$: $x_{calc}^{0} = 2.72$ with $\Delta H_{calc} = -76$ kJ/mole H_2 relative to the elemental constituents, and $x_{calc}^{max} \sim 7$ the same as for the other hydrides. We are aware of only one attempt to prepare that material. Reilly and Wiswall [13] hydrided an alloy of nominal composition $LaFe_5$ and formed a solid having the overall composition $LaFe_5H_{2.6}$ with a dissociation pressure less than 1 bar at 100 °C. No X-ray diffraction or other measurements were performed. The possibility exists that the sample comprised LaH_2, LaH_3, and Fe metal, and in our opinion verification of ternary hydride formation is warranted.

Table 2
Hydrogen contents x and enthalpies of formation ΔH of $LaTM_5H_n$ hydrides calculated via Eq. (2), as described in text, and experimental values

	$LaNi_5H_x$	$LaCo_5H_x$	$LaFe_5H_x$
x_{calc}^{0}	5.73	4.97	2.72
x_{expt}^{0}	6.2[a] 6.33[b]	3.4[d,e]	2.6[g]
$\Delta H_{calc}(x_{calc}^{0})$	−17	−36	−76
$\Delta H_{expt}(x_{expt}^{0})$	−32.1[a] −34.8[b]	−45.2[d] −43.0[e]	
$\Delta H_{calc}(x_{expt}^{0})$	−16.6 ($x = 6.2$) −16.4 ($x = 6.33$)	−30	−76
x_{calc}^{max}	6.57	6.72	6.92
x_{expt}^{max}	8.0[c]	9[f]	–
$\Delta H_{calc}(x_{calc}^{max})$	−16	−31	−56
$\Delta H_{calc}(x_{expt}^{max})$	−11	−18	–

All ΔH entries in kJ/mole H_2.

[a] Ref. [2].

[b] Ref. [8].

[c] Ref. [9]; 70 bar, 135 K.

[d] Ref. [10].

[e] Ref. [11].

[f] Ref. [12]; 1500 bar, 295 K.

[g] Ref. [13].

3. Density functional theory

3.1. Calculational methods

Electronic total energies were calculated with the Vienna *ab initio* simulation package (VASP), which implements DFT [14] using a plane wave basis set [15,16]. Projector-augmented wave potentials [17] constructed with the Perdew–Wang [18,19] generalized gradient approximation (GGA) for the exchange-correlation energy functional were employed for the atomic constituents. A plane wave cutoff energy of at least 700 eV was imposed in all cases. Lattice parameters were determined via full cell optimizations of the relevant structures. The energy of a free H_2 molecule was obtained from a calculation for a hydrogen dimer in a 11 Å × 12 Å × 13 Å orthorhombic cell.

Phonon dispersion relations for the solids and the H_2 vibrational frequency were computed with the direct method [20,21] using VASP as the computational engine. This involves construction of series of supercells, in each of which a single atom is displaced in such a way that all degrees of freedom of every symmetry-unique atomic site are explored. Each supercell was built from the VASP-optimized GGA crystal structure and made large enough to ensure that (i) interactions between equivalent atoms in periodic images were negligible and (ii) the possibility of soft modes was adequately explored. Atomic displacements of ±0.01 Å were employed in all cases.

3.2. Parent intermetallics

$LaNi_5$ and $LaCo_5$ both crystallize in the hexagonal $CaCu_5$-type P6/mmm structure. $LaNi_5$ is paramagnetic with an exchange-enhanced magnetic susceptibility, while $LaCo_5$ is a ferromagnet (Curie temperature $T_c \sim 840$ K, magnetic moment $\mu \sim 7.2\ \mu_B/LaCo_5$). We previously reported the electronic structures and ΔH results obtained from the electronic total energies [22–25]. Fig. 1 displays the phonon dispersion relations $\omega_{\vec{q}}$ and the corresponding phonon density of states calculated here for P6/mmm $LaNi_5$. There is no evidence for any structural insta-

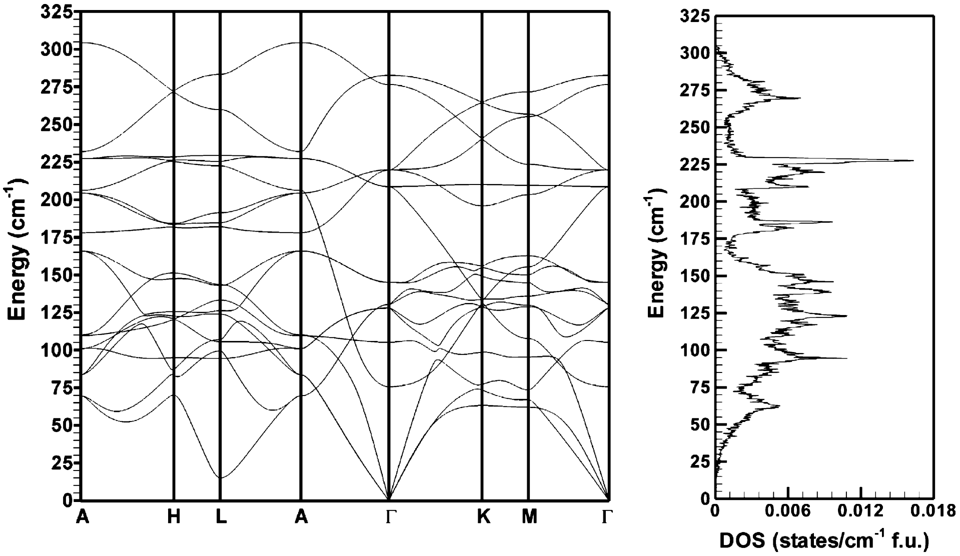

Fig. 1. Phonon dispersion curves (left panel) and phonon density of states (DOS; right panel) for hexagonal P6/mmm $LaNi_5$ calculated using a 2 × 2 × 3 supercell (72 atoms).

bility since all frequencies are real and positive. Furthermore, all $\omega_{\vec{q}} \to 0$ modes are linear in the vicinity of the Γ-point, consistent with our previous finding of positive elastic constants [22] (and elastic stability since the eigenvalues of the calculated $LaNi_5$ elastic constant matrix in ref. [22] are all positive). The zero point energy $E_{ZPE} = \frac{1}{2}\sum_{\vec{q}}\hbar\omega_{\vec{q}}$ is 17.0 kJ/mole $LaNi_5$.

Phonon results for paramagnetic P6/mmm $LaCo_5$ are strikingly different, as Fig. 2(a) shows. There are soft modes (imaginary ω plotted as negative) with large $|\omega|$, clearly pointing to structural instability. A ferromagnetic calculation yielded similar gross anomalies. Although the computations of the electronic energies for the P6/mmm structure converged with no difficulty, the phonon energies are a more sensitive measure of lattice stability, in this case at least qualitatively reflecting the breakdown of P6/mmm $LaCo_5$ as indicated by the observed eutectoid decomposition [4] mentioned previously. Analysis of the imaginary frequency modes in the vicinity of the A-point suggested an orthorhombic Cccm crystal structure. VASP optimization of that structure yielded the lattice parameters given in Table 3 and a total energy $E_{el} = -40.190$ eV/$LaCo_5$, slightly lower than $E_{el} = -40.144$ eV/$LaCo_5$ for the P6/mmm structure; the magnetic moments are both 6.7 μ_B/$LaCo_5$. The orthorhombic Cccm variant departs marginally from hexagonal lattice symmetry since $a/b\sqrt{3} = 0.990$, a ratio that would be precisely unity for a hexagonal structure described as C-centered othorhombic (cf. refs. [10,26]). Phonon calculations for the ferromagnetic Cccm structure, Fig. 2(b), exhibit no anomalies; $E_{ZPE} = 15.1$ kJ/mole $LaCo_5$.

We write the standard enthalpy of formation ΔH_T at temperature T as

$$\Delta H_T = \Delta H_0 + \delta\Delta H_T \tag{4}$$

where the zero temperature limit

$$\Delta H_0 = \Delta H_{el} + \Delta H_{ZPE} \tag{5}$$

consists of the electronic (ΔH_{el}) and zero point energy (ΔH_{ZPE}) contributions, and $\delta\Delta H_T$ represents the correction to finite temperature. The pV terms have been omitted since the small molar volumes of the solids make pV negligible at $p = 1$ bar. For the specific example of $LaNi_5$ the components of ΔH_T are

$$\Delta H_{el}(LaNi_5) = E_{el}(LaNi_5) - E_{el}(La) - 5E_{el}(Ni) \tag{6}$$

$$\Delta H_{ZPE}(LaNi_5) = E_{ZPE}(LaNi_5) - E_{ZPE}(La) - 5E_{ZPE}(Ni) \tag{7}$$

and

$$\delta\Delta H_T(LaNi_5) = E_{ph}(LaNi_5) - E_{ph}(La) - 5E_{ph}(Ni) \tag{8}$$

E_{el} is the electronic total energy from the VASP optimization. The phonon energy E_{ph} at T is

$$E_{ph} = \sum_{\vec{q}}\hbar\omega_{\vec{q}}\,n(\omega_{\vec{q}}) \tag{9}$$

Table 3
Lattice parameters and magnetic moments for orthorhombic $LaCo_5$ (Cccm; No. 66) and orthorhombic $LaCo_5H_4$ (Cmm2; No 35) structures identified from phonon calculations

	$LaCo_5$ Cccm		$LaCo_5H_4$ Cmm2	
a (Å)	8.691		8.862	
b (Å)	5.066		5.374	
c (Å)	7.885		4.090	
V (Å^3/fu)	86.79		97.39	
	Co (8k) z	0.2605	La (2a) z	0.0086
	Co (8l) x	0.3380	Co (2b) z	0.4917
	y	0.0328	Co (4c) z	0.4959
			Co (4d) x	0.3643
			z	−0.0134
			H (4c) z	0.0705
			H (4d) x	0.1457
			z	0.5124
μ (μ_B/fu)	6.7		5.8	

The sites in the Cccm $LaCo_5$ lattice are La (4c), Co (4b, 8k, 8l). In Cmm2 $LaCo_5H_4$ the sites are La (2a); Co (2b, 4c, 4d); H (4c, 4d). Only position coordinates not fixed by the space group are listed.

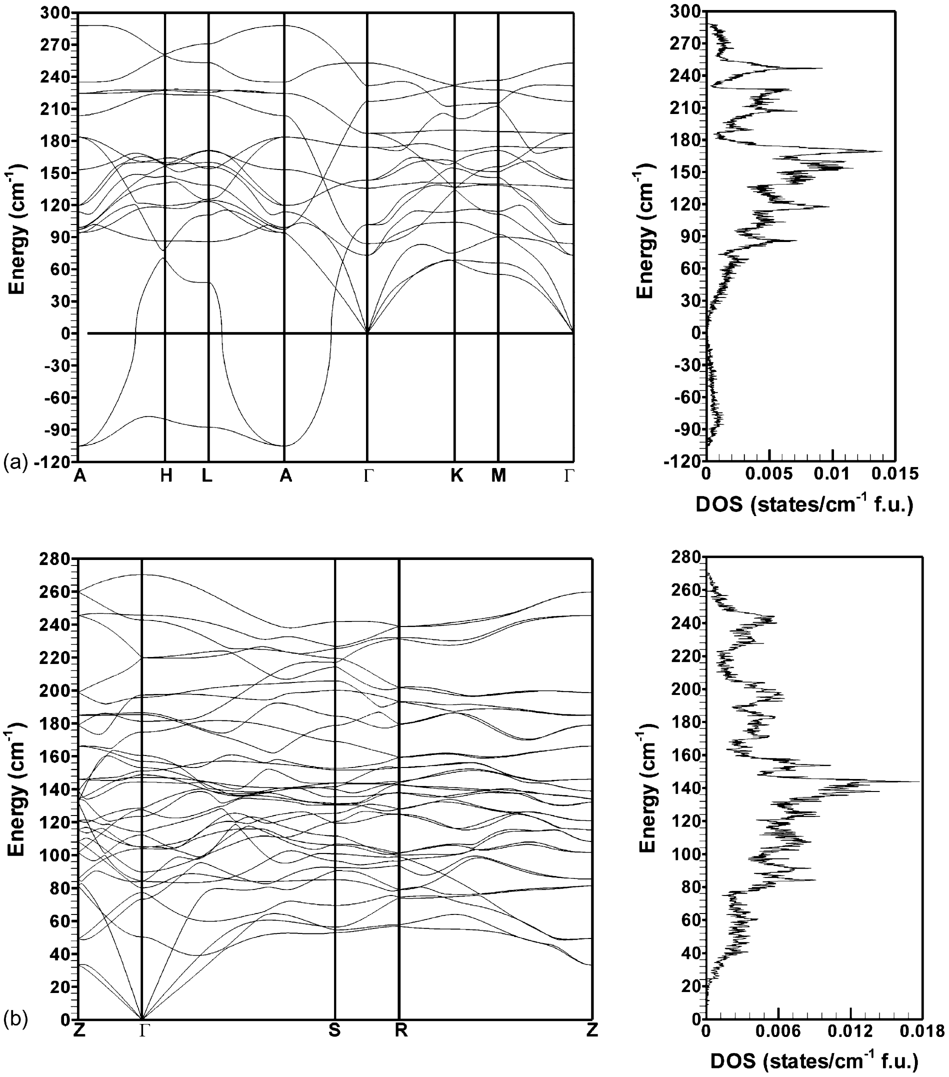

Fig. 2. Phonon dispersion curves (left panel) and phonon density of states (DOS; right panel) for (a) paramagnetic, hexagonal P6/mmm $LaCo_5$ calculated using a $2 \times 2 \times 2$ supercell (48 atoms); (b) ferromagnetic, orthorhombic Cccm $LaCo_5$ computed with a 48-atom $2 \times 1 \times 1$ supercell.

without the ZPE; $n(\omega) = (e^{\hbar\omega/kT} - 1)^{-1}$ is the Bose factor. The ZPEs from our phonon calculations for paramagnetic La ($3 \times 3 \times 1$ 36-atom supercell), ferromagnetic Ni ($2 \times 2 \times 2$ 32-atom supercell), and ferromagnetic Co ($3 \times 3 \times 2$ 36-atom supercell) are 1.09, 3.16, and 3.65 kJ/mole, respectively.

Table 4 presents the components of ΔH_{298} for $LaNi_5$ and $LaCo_5$. The E_{ZPE} terms for $LaNi_5$ very nearly cancel, as do the phonon energies E_{ph}, so that ΔH_{ZPE}, $\delta\Delta H_{298} \sim 0$ and $\Delta H_{298} \cong \Delta H_{el} = -168$ kJ/mole $LaNi_5$, which agrees well with the measured values in Table 1. For $LaCo_5$ ΔH_{ZPE} and $\delta\Delta H_{298}$ are appreciable but of opposite sign; their sum contributes -1.2 kJ/mole $LaCo_5$ to $\Delta H_{298} = -14$ kJ/mole $LaCo_5$ and serves to improve the correspondence with experiment (Table 1). We note that E_{el} (E_{ZPE}) for the P6/mmm (Cccm) structure was employed in deriving the $LaCo_5$ results in Table 4. Use of E_{el}(Cccm) would lower ΔH_{298} to -18 kJ/mole $LaCo_5$, in closer proximity to the experimental value of -17 kJ/mole $LaCo_5$, but we believe the choice of E_{el}(P6/mmm) is more appropriate since that structure is observed.

Table 4
Components of the calculated $T = 298$ K enthalpies of formation ΔH_{298} for $LaNi_5$, $LaNi_5H_7$, $LaCo_5$, and $LaCo_5H_4$ (orthorhombic Cmm2 structure)

	$LaNi_5$	$LaNi_5H_7$	$LaCo_5$	$LaCo_5H_4$
ΔH_{el}	−168.0	−39.3	−12.6[a]	−47.1
ΔH_{ZPE}	0.1	9.9	−4.2[b]	10.8
ΔH_0	−167.9	−29.3	−16.8	−36.3
$\delta\Delta H_{298}$	−0.01	−6.8	3.0	−8.2
ΔH_{298}	−167.9	−36.2	−13.8	−44.5

$LaNi_5$ and $LaCo_5$ entries in kJ/mole fu; hydride entries in kJ/mole H_2.

[a] $E_{el}(LaCo_5)$ computed for hexagonal P6/mmm structure.

[b] $E_{ZPE}(LaCo_5)$ computed for orthorhombic Cccm structure.

To explore $LaFe_5$ formation we selected as prototypes four distinct structures characterizing related compounds: (i) hexagonal P6/mmm ($LaNi_5$), (ii) hexagonal P6$_3$mc ($LaNi_5H_7$), (iii) orthorhombic Cmmm ($LaCo_5H_4$), and (iv) orthorhombic Cccm ($CeCo_5H_3$). Lanthanum was placed on the rare-earth sites and Fe on the TM sites. We find $\Delta H_{el} = +35.8 \pm 0.1$ kJ/mole $LaFe_5$ in each instance. The optimized crystal structures are quite similar, with both orthorhombic lattices very nearly hexagonal. While

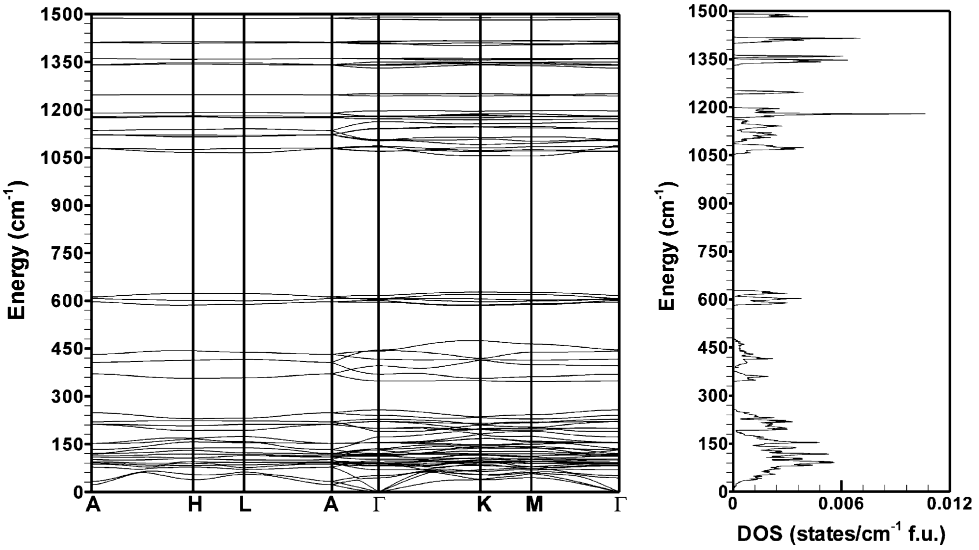

Fig. 3. Phonon dispersion curves (left panel) and phonon density of states (DOS; right panel) for hexagonal P6$_3$mc $LaNi_5H_7$ calculated using the 26-atom conventional cell. Larger supercells produced no essential differences.

our search is clearly not exhaustive, the positive values are in accord with the nonexistence of an $LaFe_5$ intermetallic phase and consistent with the result from Miedema's model in Table 1.

3.3. Hydrides

In earlier work we discussed the electronic structure and ΔH_{el} results for $LaNi_5H_7$ (hexagonal P6$_3$mc structure) [22] and $LaCo_5H_4$ (orthorhombic Cmmm structure) [23,25]. $LaNi_5H_7$ is paramagnetic, while $LaCo_5H_4$ is a ferromagnet ($T_c > 300$ K, magnetic moment $\mu \sim 5.8\,\mu_B/LaCo_5H_4$). Additionally, we derived ΔH_{el} for a large variety of filled hydrogen site configurations in those structures [24] and found that DFT identifies the 2b6c$_1$6c$_2$ (4e4h) sites in the P6$_3$mc $LaNi_5H_n$ (Cmmm $LaCo_5H_n$) structure as those occupied by hydrogen in the most stable hydride (i.e., the hydride in equilibrium with the parent intermetallic and H_2 gas at the lowest pressure), in precise agreement with neutron diffraction experiments. Maximum hydrogen contents $n \sim 11$ ($n \sim 16$) for $LaNi_5H_n$ ($LaCo_5H_n$) were estimated, somewhat greater than those from Miedema's model (Table 2) and in qualitative correspondence with the observation of $LaNi_5H_8$ at $p = 70$ bar, $T = 135$ K [9] and $LaCo_5H_9$ at $p = 1500$ bar, $T = 295$ K [12].

Here we consider the phonon spectra. Fig. 3 displays $\omega_{\vec{q}}$ calculated for $LaNi_5H_7$. As for $LaNi_5$, there is no evidence for any structural anomalies. All frequencies are positive, and the $\omega_{\vec{q}} \to 0$ branches approach the Γ-point with linear slopes and are thus consistent with our results for the elastic constants [22] that also confirm elastic stability. The zero point energy is $E_{\mathrm{ZPE}} = 143.8$ kJ/mole $LaNi_5H_7$. The situation is quite different for the orthorhombic Cmmm structure of $LaCo_5H_4$. The calculated phonon dispersion relations (Fig. 4(a)) contain imaginary modes implying instability, even though our electronic structure and elastic constant work [23,25] do not. Analysis of the imaginary modes suggested hydrogen atom displacements leading to the orthorhombic Cmm2 space group with La (2a), Co (2b, 4c, 4d), and H (4c, 4d) sites. VASP-optimized lattice parameters for that structure are listed in the final column of Table 3. The total energy $E_{\mathrm{el}} = -54.722$ eV/$LaCo_5H_4$ is slightly lower than $E_{\mathrm{el}} = -54.679$ eV/$LaCo_5H_4$ for the Cmmm structure; the magnetic moment is $5.8\,\mu_B/LaCo_5H_4$, the same as the experimental value [10], versus $6.1\,\mu_B/LaCo_5H_4$ for the Cmmm structure. The cell volume (cell constants) differs from those we determined for the Cmmm structure [23] by 0.2% (at most 1.6%). The H(4c; $x \equiv y \equiv (1/4)$, $z = 0.071$), H(4d; $x = 0.146$, $y \equiv 0$, $z = 0.512$) sites in the Cmm2 structure (Table 3) are the analogs of the H(4e;$x \equiv y \equiv (1/4)$, $z \equiv 0$), H(4h; $x = 0.148$, $y \equiv 0$, $z \equiv (1/2)$) sites in the Cmmm structure (Table 2 of ref. [23]), respectively; the displacements are quite small. The phonon spectra calculated for Cmm2 $LaCo_5H_4$ (Fig. 4(b)) exhibit no anomalies. Interpretation of the neutron diffraction data in terms of the Cmmm structure was originally made on the basis of simplicity; the authors reported that an equally accurate description could be provided by the *Cmm*2 space group [10,26]. This fact and our phonon results are cogent evidence that the Cmm2 structure (Table 3) is preferable.

We express the enthalpy of hydride formation for $LaNi_5H_7$ and $LaCo_5H_4$ again using Eqs. (4) and (5) but with respect to the parent binary and H_2 gas. In the case of $LaNi_5H_7$ we have

$$\Delta H_{\mathrm{el}}(LaNi_5H_7) = E_{\mathrm{el}}(LaNi_5H_7) - E_{\mathrm{el}}(LaNi_5) - (7/2)E_{\mathrm{el}}(H_2) \qquad (10)$$

$$\Delta H_{\mathrm{ZPE}}(LaNi_5H_7) = E_{\mathrm{ZPE}}(LaNi_5H_7) - E_{\mathrm{ZPE}}(LaNi_5) - (7/2)E_{\mathrm{ZPE}}(H_2) \qquad (11)$$

and

$$\delta\Delta H_T(LaNi_5H_7) = E_{\mathrm{ph}}(LaNi_5H_7) - E_{\mathrm{ph}}(LaNi_5) - \frac{7}{2}\left[\frac{7}{2}kT + E_{\mathrm{vib}}(H_2)\right] \qquad (12)$$

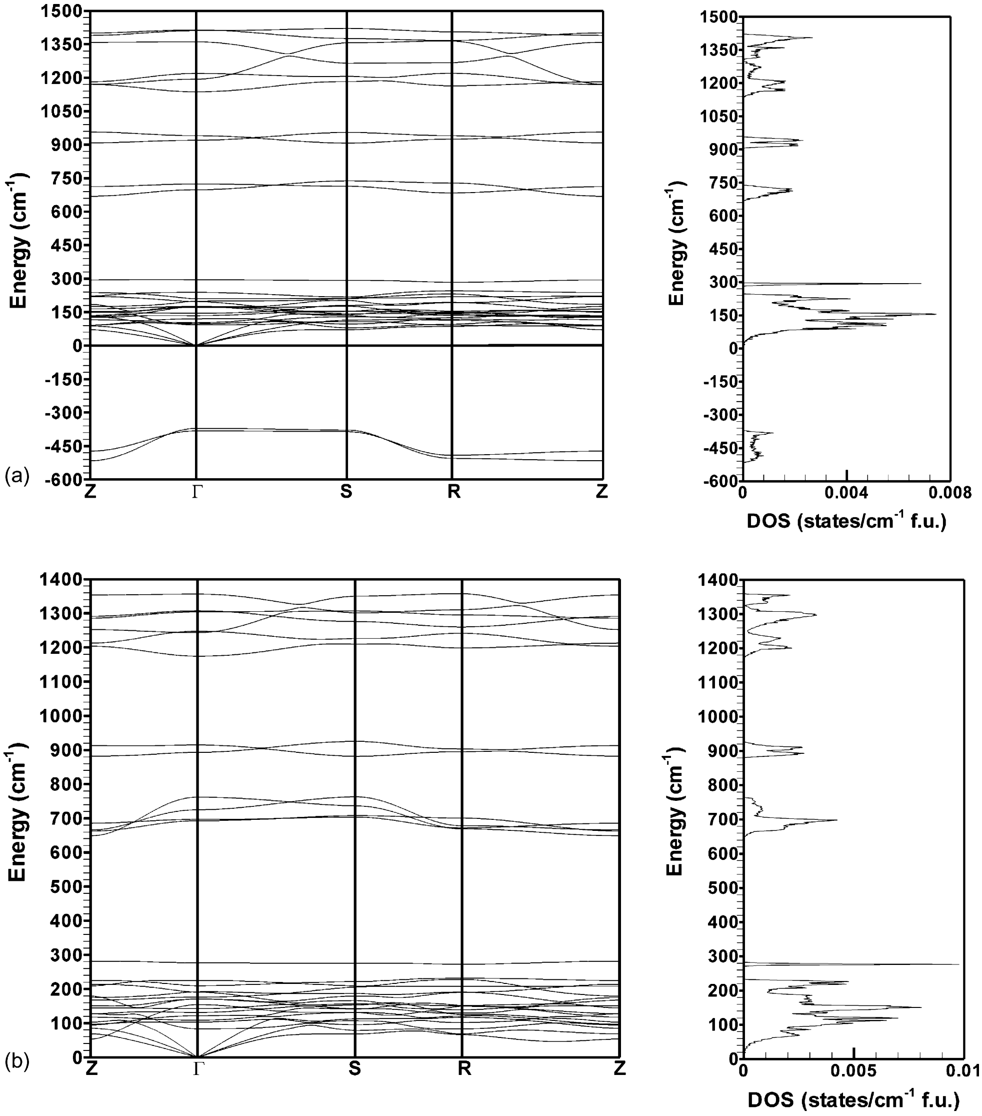

Fig. 4. Phonon dispersion curves (left panel) and phonon density of states (DOS; right panel) for ferromagnetic, orthorhombic (a) Cmmm $LaCo_5H_4$; (b) Cmm2 $LaCo_5H_4$. A 40-atom 1 × 1 × 2 supercell was employed in each case.

where $(7/2)kT$ is the sum of the translational $(3/2kT)$, rotational (kT), and $pV = kT$ terms for the H_2 molecule and $E_{\mathrm{vib}} = \hbar\omega_0 n(\omega_0)$ its vibrational energy (we calculate $\omega_0(H_2) = 4399\,\mathrm{cm}^{-1}$, in excellent accord with the measured value of $4405\,\mathrm{cm}^{-1}$ [27]). Table 4 includes results for ΔH_{298} of $LaNi_5H_7$ and $LaCo_5H_4$. In each case $[\Delta H_{\mathrm{ZPE}} + \delta\Delta H_{298}]$ is positive and serves to bring ΔH_{298} closer to experiment (Table 2) than the electronic component ΔH_{el} alone. The DFT values are also substantially more accurate than those from Miedema's model in Table 2.

Our preliminary findings suggest that a $LaFe_5H_n$ hydride forms. We have calculated

$$\Delta H_{\mathrm{el}}(\mathrm{LaFe_5H}_n) = E_{\mathrm{el}}(\mathrm{LaFe_5H}_n) - E_{\mathrm{el}}(\mathrm{La}) - 5E_{\mathrm{el}}(\mathrm{Fe}) - \tfrac{n}{2}E_{\mathrm{el}}(\mathrm{H_2}) \qquad (13)$$

the electronic component of the enthalpy of formation with respect to the elemental metals and H_2 gas, for a broad range of hydrogen site configurations in the same four structures explored for $LaFe_5$ (Section 3.2). To this point the most negative ΔH_{el} values we have obtained are −24.6, −34.8, −35.2, and −38.7 kJ/mole H_2 for P6/mmm $LaFe_5H_{12}$ (12o), $P6_3mc$ $LaFe_5H_7$ ($2b6c_16c_2$), Cmmm $LaFe_5H$ (4h), and Cccm $LaFe_5H_7$ (4e8g16m), respectively, where the occupied H sites are in parentheses. The orthorhombic Cccm structure thus appears most favorable. Additional configurations will be investigated, and we will calculate the elastic properties and phonon spectrum of the most stable hydride.

4. Summary

We have shown that Miedema's semiempirical model correctly accounts for the most fundamental characteristics of the $La(TM)_5H_n$ (TM = Fe, Co, Ni) materials, namely: (i) the formation of $LaNi_5$, $LaCo_5$, and hydrides of them; and (ii) the absence of $LaFe_5$ and other La–Fe binary compounds. The model also predicts the formation of a $LaFe_5$ hydride, underscoring its utility as at least a qualitative tool for determining the existence of novel hydrides when no other information is available.

Our first principles DFT work confirms the general predictions of Miedema's model and provides more accurate results for the enthalpies of formation. DFT enables, of course, the calculation of electronic and vibrational properties beyond the scope of Miedema's construct, including the zero point and finite temperature contributions to ΔH, hydrogen site preferences, and magnetic moments. For $LaCo_5$ and $LaCo_5H_4$ we have demonstrated that computation of the phonon spectra can yield important inferences with regards to the crystal structure and structural stability. To our knowledge the phonon spectra in Figs. 1–4 have neither been measured nor previously calculated.

Acknowledgements

We are grateful to G.P. Meisner, M.S. Meyer, and F.E. Pinkerton for productive discussions.

References

[1] F.R. de Boer, R. Boom, W.C.M. Mattens, A.R. Miedema, A.K. Niessen, in: F.R. de Boer, D.G. Pettifor (Eds.), Cohesion and Structure, vol. 1, North-Holland, Amsterdam, 1988.
[2] W.N. Hubbard, P.L. Rawlins, P.A. Connick, R.E. Stedwell Jr., P.A.G. O'Hare, J. Chem. Thermodyn. 15 (1983) 785.
[3] C. Colinet, A. Pasturel, A. Percheron-Guegan, J.C. Achard, J. Less Common Met. 134 (1987) 109.
[4] K.H.J. Buschow, J. Less Common Met. 29 (1972) 283.
[5] P.C.P. Bouten, A.R. Miedema, J. Less Common Met. 71 (1980) 147.
[6] J.F. Herbst, J. Alloys Compd. 337 (2002) 99.
[7] K.H.J. Buschow, in: K.A. Gschneidner Jr., L. Eyring (Eds.), Handbook on the Physics and Chemistry of Rare Earths, vol. 6, North-Holland, Amsterdam, 1984, p. 1.
[8] J.J. Murray, M.L. Post, J.B. Taylor, J. Less Common Met. 80 (1981) 211.
[9] V.N. Verbetskii, V.A. Pil'chenko, S.S. Kashkadov, K.N. Semenenko, Russ. J. Inorg. Chem. 29 (1984) 2188.
[10] F.A. Kuijpers, Philips Res. Repts. Suppl. (1973) (No. 2).
[11] T.B. Flanagan, S. Majorowski, J.D. Clewley, C.-N. Park, J. Less Common Met. 103 (1984) 93.
[12] J.F. Lakner, F.S. Uribe, S.A. Steward, J. Less Common Met. 74 (1980) 13 (Lawrence Livermore Laboratory Rept. UCRL-52039, 1976).
[13] J.J Reilly, R.H Wiswall Jr., Brookhaven National Laboratory Report BNL 17136, August 1, 1972.
[14] W. Kohn, L. Sham, Phys. Rev. 140 (1965) A1133.
[15] G. Kresse, J. Hafner, Phys. Rev. B 49 (1994) 14251.
[16] G. Kresse, J. Furthmüller, Comput. Mater. Sci. 6 (1996) 15.
[17] P.E. Blöchl, Phys. Rev. B 50 (1994) 17953.
[18] J.P. Perdew, Y. Wang, Phys. Rev. B 45 (1992) 13244.
[19] J.P. Perdew, J.A. Chevary, S.H. Vosko, K.A. Jackson, M.R. Pederson, D.J. Singh, C. Fiolhais, Phys. Rev. B 46 (1992) 6671.
[20] J. Lazewski, P.T. Jochym, K. Parlinski, J. Chem. Phys. 117 (2002) 2726.
[21] K. Parlinski, J. Alloys Compd. 328 (2001) 97.
[22] L.G. Hector Jr., J.F. Herbst, T.W. Capehart, J. Alloys Compd. 353 (2003) 74 ($LaNi_5$, $LaNi_5H_7$).
[23] L.G. Hector Jr., J.F. Herbst, Appl. Phys. Lett. 82 (2003) 1042 [RCo_5, RCo_5H_4 (R = La, Pr)].
[24] J.F. Herbst, L.G. Hector Jr., Appl. Phys. Lett. 85 (2004) 3465 ($LaNi_5H_n$, $LaCo_5H_n$).
[25] L.G. Hector Jr., J.F. Herbst, J. Alloys Compd. 379 (2004) 41 [RCo_5H_n (R = La, Ce, Pr)].
[26] F.A. Kuijpers, B.O. Loopstra, J. Phys. Chem. Solids 35 (1974) 301.
[27] G. Herzberg, Molecular Spectra and Molecular Structure, I. Diatomic Molecules, Prentice-Hall, New York, 1939.